



**HAL**  
open science

## Measurement of absolute $\gamma$ -ray emission probabilities in the decay of $^{227}\text{Ac}$ in equilibrium with its progeny

M. Marouli, G. Lutter, S. Pommé, R. van Ammel, M. Hult, Sylvie Pierre, P. Dryák, P. Carconi, A. Fazio, F. Bruchertseifer, et al.

### ► To cite this version:

M. Marouli, G. Lutter, S. Pommé, R. van Ammel, M. Hult, et al.. Measurement of absolute  $\gamma$ -ray emission probabilities in the decay of  $^{227}\text{Ac}$  in equilibrium with its progeny. Applied Radiation and Isotopes, 2019, 144, pp.34-46. 10.1016/j.apradiso.2018.08.023 . cea-04550280

**HAL Id: cea-04550280**

**<https://cea.hal.science/cea-04550280>**

Submitted on 17 Apr 2024

**HAL** is a multi-disciplinary open access archive for the deposit and dissemination of scientific research documents, whether they are published or not. The documents may come from teaching and research institutions in France or abroad, or from public or private research centers.

L'archive ouverte pluridisciplinaire **HAL**, est destinée au dépôt et à la diffusion de documents scientifiques de niveau recherche, publiés ou non, émanant des établissements d'enseignement et de recherche français ou étrangers, des laboratoires publics ou privés.



Distributed under a Creative Commons Attribution 4.0 International License



# Measurement of absolute $\gamma$ -ray emission probabilities in the decay of $^{227}\text{Ac}$ in equilibrium with its progeny

M. Marouli<sup>a,\*</sup>, G. Lutter<sup>a</sup>, S. Pommé<sup>a</sup>, R. Van Ammel<sup>a</sup>, M. Hult<sup>a</sup>, S. Pierre<sup>b</sup>, P. Dryák<sup>c</sup>, P. Carconi<sup>d</sup>, A. Fazio<sup>d</sup>, F. Bruchertseifer<sup>e</sup>, A. Morgenstern<sup>e</sup>

<sup>a</sup> European Commission, Joint Research Centre, Directorate for Nuclear Safety and Security, Retieseweg 111, B-2440 Geel, Belgium

<sup>b</sup> CEA, LIST, Laboratoire National Henri Becquerel (LNE-LNHB), Bât. 602 PC111 CEA Saclay, F-91191 Gif-sur-Yvette, France

<sup>c</sup> Český Metrologický Institut, Radiová 1, 102 00 Praha 10, Czech Republic

<sup>d</sup> ENEA, Istituto Nazionale di Metrologia delle Radiazioni Ionizzanti, C.R. Casaccia, P.O. Box 2400, I-00100 Rome A.D., Italy

<sup>e</sup> European Commission, Joint Research Centre, Directorate for Nuclear Safety and Security, Hermann-von-Helmholtz-Platz 1, 76344 Eggenstein-Leopoldshafen, Germany

## HIGHLIGHTS

- Measured gamma-ray emission probabilities in  $^{227}\text{Ac}$  decay series.
- Mean values taken from 4 laboratories.
- Source activity determined by primary standardisation.
- Results reported for 87  $\gamma$ -ray lines.
- Generally in good agreement with literature values.

## ARTICLE INFO

### Keywords:

$\gamma$ -ray intensities

$^{227}\text{Ac}$

$^{227}\text{Th}$

$^{223}\text{Ra}$

Decay data

$\gamma$ -ray spectrometry

## ABSTRACT

The emission probabilities of  $\gamma$  rays produced in the  $^{227}\text{Ac}$  decay series were determined by high-resolution  $\gamma$ -ray spectrometry of sources with standardised activity. The sources were prepared quantitatively on glass discs by drop deposition of a solution with  $^{227}\text{Ac}$  in radioactive equilibrium with its daughter nuclides. Their activity was measured by a primary standardisation technique based on alpha-particle counting at a defined low solid angle. Four laboratories performed  $\gamma$ -ray spectrometry and derived absolute  $\gamma$ -ray intensities. Mean values were calculated and compared with literature data and the currently recommended evaluated data. New values on certain  $\gamma$ -ray emission probabilities are proposed.

## 1. Introduction

The  $^{227}\text{Ac}$  decay series has been the subject of increased metrological interest in recent years. Firstly, it is part of the  $^{235}\text{U}$  decay chain, which is ubiquitously present in nature and considered a health risk where industry processing natural resources enhances the concentration of natural occurring radionuclides (NOR) in its products, by-products and waste. Of particular concern are the alpha decays from  $^{227}\text{Ac}$  and progeny at the end of the  $^{235}\text{U}$  decay chain, which can cause a high internal dose after incorporation in the human body. Secondly, the daughter nuclides  $^{227}\text{Th}$  and  $^{223}\text{Ra}$  and their progeny are becoming

increasingly important for radioimmunotherapy (Seidl, 2014). The capacity of alpha particles to cause DNA double-strand breaks which trigger cell death can be successfully applied in treatment of disseminated cancer cells and small tumour cell clusters (Humm et al., 2015; Kratochwil et al., 2016).

Accurate decay data of the  $^{227}\text{Ac}$  decay series are needed to provide the necessary metrological tools to verify exemption levels in the NORM industry (EURATOM, 2014) by  $\gamma$ -ray spectrometry and to calibrate ionisation chambers for the quantified therapeutic use of  $^{227}\text{Th}$ ,  $^{223}\text{Ra}$  in nuclear medicine. In recent work, improved  $\gamma$ -ray intensities in the decay of  $^{235}\text{U}$  have been published in support of SI-

\* Corresponding author.

E-mail addresses: [Maria.MAROULI@ec.europa.eu](mailto:Maria.MAROULI@ec.europa.eu) (M. Marouli), [Guillaume.LUTTER@ec.europa.eu](mailto:Guillaume.LUTTER@ec.europa.eu) (G. Lutter), [Stefaan.POMME@ec.europa.eu](mailto:Stefaan.POMME@ec.europa.eu) (S. Pommé), [Raf.VAN-AMMEL@ec.europa.eu](mailto:Raf.VAN-AMMEL@ec.europa.eu) (R. Van Ammel), [Mikael.HULT@ec.europa.eu](mailto:Mikael.HULT@ec.europa.eu) (M. Hult), [sylvie.pierre@cea.fr](mailto:sylvie.pierre@cea.fr) (S. Pierre), [pdryak@cmi.cz](mailto:pdryak@cmi.cz) (P. Dryák), [pierluigi.carconi@enea.it](mailto:pierluigi.carconi@enea.it) (P. Carconi), [aldo.fazio@enea.it](mailto:aldo.fazio@enea.it) (A. Fazio), [Frank.BRUCHERTSEIFER@ec.europa.eu](mailto:Frank.BRUCHERTSEIFER@ec.europa.eu) (F. Bruchertseifer), [Alfred.MORGENSTERN@ec.europa.eu](mailto:Alfred.MORGENSTERN@ec.europa.eu) (A. Morgenstern).

<https://doi.org/10.1016/j.apradiso.2018.08.023>

Received 20 March 2018; Received in revised form 27 July 2018; Accepted 28 August 2018

Available online 30 August 2018

0969-8043/© 2018 The Authors. Published by Elsevier Ltd. This is an open access article under the CC BY license (<http://creativecommons.org/licenses/by/4.0/>).

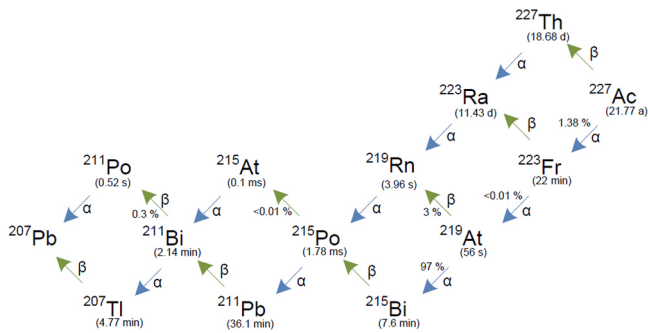


Fig. 1. The decay series of  $^{227}\text{Ac}$ .

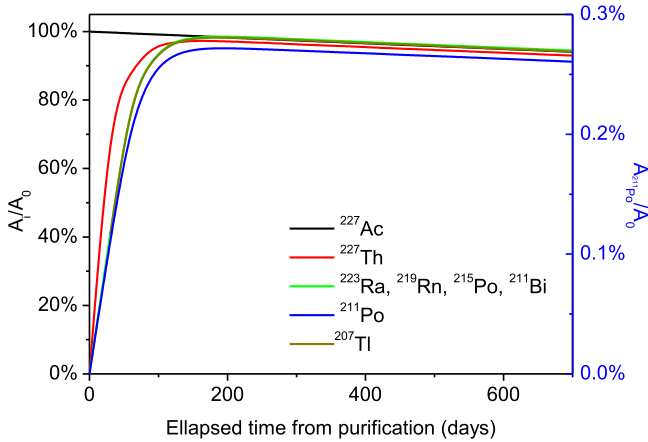


Fig. 2. Theoretical relative activities in the  $^{227}\text{Ac}$  decay chain.  $A_0$  is the initial  $^{227}\text{Ac}$  activity and  $A_i$  the activity of the decay product.

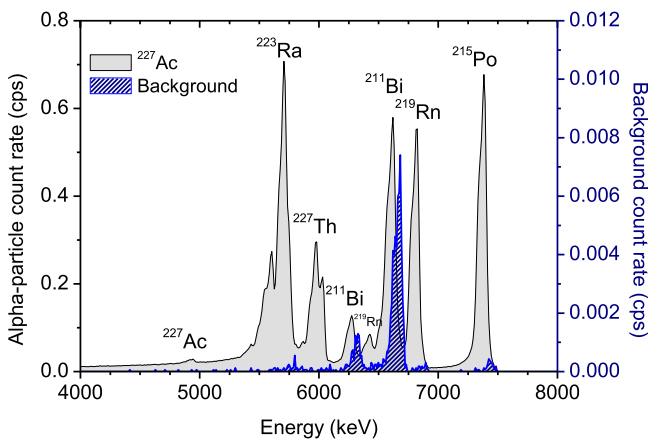


Fig. 3. Alpha-particle spectra of a  $^{227}\text{Ac}_{\text{eq}}$  source and a background spectrum with decays from recoiled atoms in the PIPS<sup>®</sup> detector taken at JRC.

traceability of radiological measurements (Marouli et al., 2018), in particular in the context of NORM. Mostly in support of alpha immunotherapy, specific studies have been performed on the half-lives of  $^{227}\text{Th}$  (Collins et al., 2015c) and  $^{223}\text{Ra}$  (Bergeron and Fitzgerald, 2015; Collins et al., 2015a; Kossert et al., 2015), primary standardisation of their activity and determination of the  $\gamma$ -ray emissions in their decay

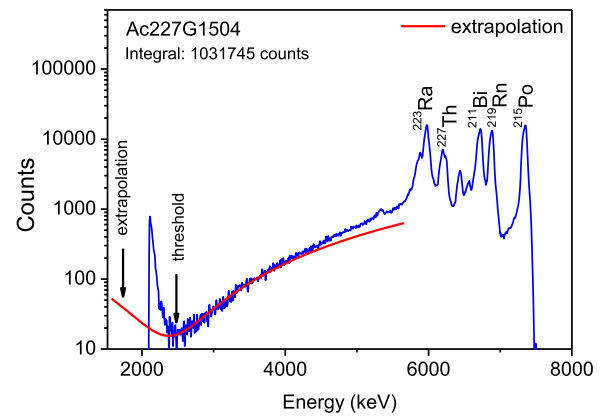


Fig. 4. Alpha spectrum of a  $^{227}\text{Ac}_{\text{eq}}$  source (Ac227G1504), measured at JRC-Geel with the defined solid angle alpha counting set-up.

Table 1  
Activity of  $^{227}\text{Ac}$  in the sources standardised by DSA alpha-particle counting and standard uncertainty ( $k = 1$ ).

Source	Activity (Bq) <sup>†</sup>
Ac227G1502	1183 (9)
Ac227G1507	1077 (7)
Ac227SS1508	945 (8)
Ac227G1509	1103 (6)

<sup>†</sup> Reference date: 17th June 2015.

Table 2  
Typical uncertainty components of the  $^{227}\text{Ac}$  activities ( $k = 1$ ).

Component	Relative uncertainty (%)
Counting statistics	0.10
Dead time (+ pile-up)	0.08
Background	0.01
Detection efficiency	0.15
Extrapolation to zero energy	0.50
Absorption	0.10
Scattering	0.02
Non-equilibrium	0.15
Impurities	0.10
<b>Total</b>	<b>0.57</b>

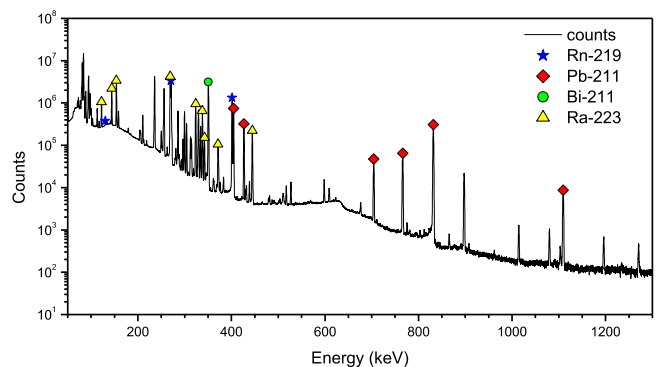


Fig. 5.  $\gamma$ -ray spectrum of a  $^{227}\text{Ac}_{\text{eq}}$  source measured at JRC-Geel. The selected  $\gamma$ -ray peaks for the estimation of the source activity are colour and shape coded.

**Table 3**  
Activity measurement of the Ac227G1509 source by  $\gamma$ -ray spectrometry.

	Ge-T5	Ge-5
<b>Radionuclide</b>		<b>Activity (Bq)</b>
<sup>223</sup> Ra	1110(50)	1077(51)
<sup>219</sup> Rn	1070(60)	1082(53)
<sup>211</sup> Pb	1115(55)	1156(57)
<sup>211</sup> Bi	1130 (60)	1145(57)
<sup>227</sup> Ac	1107 (50)	1115(51)
		<b>1110 (50)<sup>*</sup></b>

\* Power moderated mean value.

(Keightley et al., 2015; Kossert et al., 2015; Collins et al., 2015b; Zimmerman et al., 2015; Pibida, 2015), and methodology for age dating of a <sup>227</sup>Th-<sup>223</sup>Ra material (Pommé et al., 2016). In previous studies, the decay characteristics of the <sup>230</sup>U (Pommé et al., 2012a, 2012b; Marouli et al., 2012; Suliman et al., 2012) and <sup>225</sup>Ac (Pommé et al., 2012c; Marouli et al., 2013; Suliman et al., 2013) decay chains have been investigated for the same purpose.

Actinium-227 (21.77 a) decays to stable <sup>207</sup>Pb through a series of twelve alpha and beta emitters (DDEP, 2004–2016) (Fig. 1). Following the main decay path, a plethora of  $\gamma$  rays is emitted predominantly from the <sup>227</sup>Th  $\rightarrow$  <sup>223</sup>Ra and <sup>223</sup>Ra  $\rightarrow$  <sup>219</sup>Rn decays. Taking into consideration initially only evaluated nuclear decay data by the Decay Data Evaluation Project (DDEP) and Nuclear Data Sheets (NDS), <sup>227</sup>Ac decays mainly to <sup>227</sup>Th by  $\beta^-$  decay followed by  $\gamma$  rays which have not been measured directly but deduced from the absolute  $\beta^-$  emission probabilities and the total conversion coefficients (Kondev et al., 2016). Recommended  $\gamma$ -ray intensities for the <sup>227</sup>Th  $\rightarrow$  <sup>223</sup>Ra decay come from measurements dating back to 1969, with the most recent one from G. Ardisson and published in a private communication by Abdul-Hadi et al. (1993). The levels of <sup>215</sup>Po are fed from the <sup>219</sup>Rn  $\rightarrow$  <sup>215</sup>Po alpha decay. Evaluations of the  $\gamma$ -ray emission probabilities by DDEP and NDS (Lee, 2013) include results dating back to 1967. The latest one is from 1999 by Liang et al. (1999) who observed the alpha decay of <sup>219</sup>Rn and coincident  $\gamma$  rays and electrons. In many cases, the results from the different studies are not in agreement. For the only  $\gamma$  ray observed from the alpha decay of <sup>215</sup>Po, two discrepant experimental values exist at 0.048 (5) % (Briçon et al., 1968) and 0.064 (2) % (Davidson, Connor,

**Table 4**  
Experimental conditions of the  $\gamma$ -ray intensity measurements.

	JRC	ENEA	CEA	CMI
<b>Detector</b>	HPGe, Planar BEGe, Thin dead layer, Underground lab (Hades)	HPGe (p-type)	HPGe (n-type), Underground lab	HPGe
<b>FWHM</b>	0.91 keV @ 122 keV, 1.93 keV @ 1332.5 keV	0.9 keV @ 122 keV, 1.9 keV @ 1332.5 keV	0.99 keV @ 122 keV, 2.05 keV @ 1332.5 keV	1.8 keV @ 1332.5 keV
<b>Relative efficiency</b>	50 %	40 %	52 %	40 %
<b>Live time (days)</b>	41	5	4	6
<b>Source-detector distance (mm)</b>	120	100	50	100
<b>FEP Efficiency</b>	PTB point sources + EGSnrc <sup>I</sup>	GESPECOR 4.2 <sup>II</sup>	Point sources + AÇORES <sup>III</sup>	MCNP <sup>IV</sup>
<b>Coincidence corrections</b>	EGSnrc	GESPECOR 4.2	ETNA <sup>V</sup>	MCNP

<sup>I</sup> Kawrakow et al. (2015).

<sup>II</sup> Sima et al. (2001).

<sup>III</sup> LNHB (2008).

<sup>IV</sup> Goorley et al. (2012).

<sup>V</sup> Piton et al. (2000).

**Table 5**  
Absolute  $\gamma$ -ray emission probabilities measured in the <sup>227</sup>Ac  $\rightarrow$  <sup>227</sup>Th decay.

Energy (keV)	DDEP	JRC	ENEA	CEA	CMI	This work
37.9	0.049	0.050 (5)				0.050 (5)

1970). <sup>211</sup>Pb  $\rightarrow$  <sup>211</sup>Bi is a well-studied decay with values on 22  $\gamma$ -ray emission probabilities published in 12 papers. The subsequent alpha decay (99.724 %) of <sup>211</sup>Bi  $\rightarrow$  <sup>207</sup>Tl is followed by a single  $\gamma$  ray with an absolute emission probability in the most recent evaluations being calculated using the total internal conversion coefficient. The latest experimental value is provided by Momeni (1982). Both calculated (13.0 %) and experimental (13.3 %) values are in agreement. One  $\gamma$  ray is emitted in the <sup>207</sup>Tl  $\rightarrow$  <sup>207</sup>Pb  $\beta^-$  decay. The  $\gamma$ -ray intensity is deduced from the intensity ratio of the 897.77 keV <sup>207</sup>Tl  $\gamma$ -ray line to the 351 keV from the <sup>211</sup>Bi  $\rightarrow$  <sup>207</sup>Tl decay as discussed by Hindi et al. (1988).

One of the objectives of the EMRP project 'JRP IND57 MetroNORM: Metrology for processing materials with high natural radioactivity' was to improve the quality of available data for  $\gamma$ -ray emission probabilities in the decay of the <sup>227</sup>Ac and its progeny. Experimental work from the four out of the five laboratories participating in the project is presented in this paper. The fifth laboratory, Laboratorio de Metrología de Radiaciones Ionizantes CIEMAT in Spain, has withdrawn its results at the final stage for technical reasons. Most of the emission probabilities derived from this work agree with published values and uncertainties have been reduced in some cases.

## 2. Source preparation

### 2.1. Source production of <sup>227</sup>Ac

The <sup>227</sup>Ac<sub>eq</sub> (i.e., <sup>227</sup>Ac in equilibrium with its daughter products) solution was provided to JRC-Geel (JRC-IRMM before 2016) by JRC-Karlsruhe, four years after its production, (JRC-ITU before 2016) in a tip vial containing 0.5 mL (0.1 M HCl) solution with an activity of 4.5 MBq (on the reference date of March 2011). The material was originally produced by neutron irradiation of <sup>226</sup>Ra at the BR2 reactor at the Belgian nuclear research institute (SCK-CEN, 2015). The separation of

$^{227}\text{Ac}$  from  $^{226}\text{Ra}$  was performed by repeated extraction chromatography using RE resin (Apostolidis et al., 2005). The aliquot was further purified by extraction chromatography using DGA-branched resin (TEHDGA) as described by Zielinska et al. (2007).

## 2.2. Sources for activity measurement

$^{227}\text{Ac}$  had reached equilibrium with the decay products at the start of the source preparation, (Fig. 2). One of the decay products, the noble gas  $^{219}\text{Rn}$  ( $T_{1/2} \approx 4$  s), poses a risk of contamination during the handling of the material. This risk is also present when manipulating deposited open sources. Additionally, alpha-emitters gain recoil energy of roughly 100 keV during decay, which is enough for some decay products to escape from an open source and spread in the air. Safety measures were taken to reduce the risks of radiation contamination by

inhalation. To avoid possible contamination, source preparation was carried out in glove boxes.

To obtain thin sources with small crystals, the 34-mm-diameter glass source support discs were pre-treated before drop deposition. A solution of wetting agent (Tween® 1/40 diluted) and seeding agent (Ludox 1/100 diluted) was sprayed on the discs in a circular shape of 6 mm diameter using an airbrush pencil (Van Ammel et al., 2011) and dried in air. From the original solution, 20  $\mu\text{L}$  (180 kBq) was transferred to a double-sealed ampoule. Carrier solution (3.6 mL 0.1 M HCl) was added, resulting in an approximate activity concentration of 1.0 kBq/20  $\mu\text{L}$ . From this ampoule, 18 sources were prepared on the glass discs and one ( $\text{Ac}227\text{SS1508}$ ) on a 25.4 mm stainless steel disc. After the deposition, the sources were dried in open air without the aid of a heating device. The sources were subsequently covered with two VYNS (vinyl chloride vinyl acetate copolymer) foils of 35  $\mu\text{g}/\text{cm}^2$  thickness.

**Table 6**  
Absolute  $\gamma$ -ray emission probabilities (%) measured in the  $^{227}\text{Th} \rightarrow ^{223}\text{Ra}$  decay.

Energy (keV)	NDS	JRC	ENEA	CEA	CMI	This work
31.58	0.068 (12)	0.071 (6)				0.071 (6)
40.2	0.015 (4)	0.067 (5)				0.067 (5)
61.441	0.090 (13)	0.063 (5) <sup>a</sup>				0.063 (5)
62.45 + 62.68	0.21 (3)	0.16 (1)				0.16 (1)
113.11	0.70	0.82 (5) <sup>b</sup>			0.83 (5) <sup>b</sup>	0.82 (4)
117.2	0.199 (22)	0.201 (12)	0.208(12)		0.200 (13)	0.203 (9)
123.58	0.014 (5)	0.0068 (13)				0.0068 (13)
141.42	0.119 (23)	0.123 (6)			0.110 (14)	0.118 (8)
150.14	0.011 (3)	0.017 (2)				0.017 (2)
162.19	0.008 (3)	0.017 (2)				0.017 (2)
168.36	0.015 (3)	0.012 (1)				0.012 (1)
169.95	0.0055 (22)	0.008 (1)				0.008 (1)
197.56	0.013 (4)			0.0109(4)		0.0109 (5)
201.64	0.024 (3)	0.020 (2)		0.020(1)		0.020 (1)
204.14	0.23 (3)				0.200 (17)	0.200 (17)
204.98	0.16 (3)	0.336 (16)			0.151 (17)	0.151 (18)
204.14 + 204.98	0.39 (5)					0.336 (16)
206.08	0.25 (3)	0.288 (14)		0.262(7)	0.256 (11)	0.268 (13)
210.62	1.25 (14)	1.21 (6)	1.25(6)	1.20(4)	1.18 (5)	1.21 (5)
212.7 + 212.7	0.098 (13)	0.097 (5)				0.097 (5)
218.9	0.110 (14)	0.103 (5)			0.097 (15)	0.101 (6)
235.96	12.9 (11)	12.8 (6)	13.3(6)	12.8(4)	13.1 (5)	13.0 (5)
246.12	0.0123 (14)	0.021 (2) <sup>c</sup>				0.021 (2)
252.5	0.111 (18)	0.093 (5)			0.140 (8)	0.117 (24)
254.63	0.71 (14)	0.71 (4)			0.83 (3)	0.77 (7)
256.23	7.0 (6)	6.8 (4)	7.6 (4)	6.88 (18)	7.04 (22)	7.0 (3)
262.87	0.107 (12)	0.124 (6)			0.129 (15)	0.126 (6)
272.91	0.51 (4)	0.534 (25)			0.513 (18)	0.523 (21)
279.8	0.054 (14)	0.046 (2)			0.041 (5)	0.044 (3)
281.42	0.178 (19)	0.171 (8)			0.174 (8)	0.172 (8)
284.24	0.040 (13)	0.0338 (18)				0.0338 (18)
286.09	1.74 (21)	1.90 (9)	1.80 (8)	1.85 (5)	1.86 (6)	1.87 (7)
292.41	0.066 (10)	0.059 (3)				0.059 (3)
296.5	0.44 (5)	0.436 (21)		0.467 (12)	0.455 (15)	0.454 (17)
299.98 + 300.5	2.22 (20)	2.18 (10)	2.26 (10)	2.26 (6)		2.25 (8)
304.5	1.15 (16)	1.08 (5)	1.10 (5)	1.11 (3)	1.08 (4)	1.10 (4)
308.4	0.017 (3)	0.020 (1)				0.020 (1)
314.85	0.49 (6)	0.489 (23)	0.493 (22)		0.503 (18)	0.495 (18)
346.45	0.0120 (16)	0.0096 (11)				0.0096 (11)
466.8	0.00049 (5)	0.0014 (4)				0.0014 (4)

<sup>a</sup> Negligible interferences from the  $^{227}\text{Ac}$  60.6 keV  $\gamma$  ray with  $P_{\gamma} = 0.000041$  % and the  $^{223}\text{Fr}$  61.43 keV  $\gamma$  ray with  $P_{\gamma} = 0.000049$  %.

<sup>b</sup> Interference from the  $^{227}\text{Th}$  112.6 keV  $\gamma$  ray with  $P_{\gamma} = 0.009$  % has been subtracted.

<sup>c</sup> Interference from the  $^{227}\text{Th}$  245.6 keV  $\gamma$  ray with  $P_{\gamma} = 0.00027$  is considered negligible.

**Table 7**  
Absolute  $\gamma$ -ray emission probabilities (%) measured in the  $^{223}\text{Ra} \rightarrow ^{219}\text{Rn}$  decay.

Energy (keV)	DDEP	JRC	ENEA	CEA	CMI	This work
122.319	1.238 (19)	1.37 (7)	1.39 (6)		1.42 (6)	1.39 (6)
144.27	3.36 (8)	3.67 (17)			3.76 (16)	3.71 (15)
154.208	5.84 (13)	6.4 (3) <sup>d</sup>	6.40 (28) <sup>d</sup>		6.52 (21) <sup>d</sup>	6.43 (23)
158.635	0.713 (16)	0.78 (4) <sup>e</sup>	0.80 (4) <sup>e</sup>		0.80 (3) <sup>e</sup>	0.795 (30)
165.8	0.0054 (28)	0.0037 (15)				0.0037 (15)
177.3	0.047 (4)	0.055 (3)				0.055 (3)
179.54	0.154 (14)	0.186 (9)	0.168 (9)	0.155 (5)	0.133 (15)	0.161 (12)
221.32	0.036 (6)	0.030 (2)				0.0304 (19)
269.46	14.23 (32)	13.7 (7)	14.2 (6)		14.4 (5)	14.1 (5)
288.18	0.161 (5)	0.126 (6)				0.126 (6)
323.87	4.06 (9)	3.74 (18)			3.96 (13)	3.85 (17)
338.282	2.85 (6)	2.66 (13)	2.78 (12)		2.84 (9)	2.76 (10)
355.5	0.0043 (14)	0.0085 (7)				0.0085 (7)
371.68	0.499 (11)	0.445 (21)			0.468 (17)	0.457 (18)
445.03	1.28 (4)	1.25 (6) <sup>f</sup>	1.28 (6) <sup>f</sup>		1.29 (4) <sup>f</sup>	1.28 (5)
487.5	0.011 (2)	0.0064 (6)				0.0064 (6)
527.61	0.073 (4)	0.068 (3)			0.075 (15)	0.070 (4)
537.6	0.0021 (7)	0.0033 (5) <sup>g</sup>				0.0033 (5)
541.99	0.0014 (6)	0.0012 (5)				0.0012 (5)
598.721	0.092 (4)	0.087 (4)			0.083 (18)	0.086 (4)
623.68	0.009 (4)	0.007 (2) <sup>h</sup>				0.007 (2)
711.3	0.0037 (1)	0.0030 (4)				0.0030 (4)

<sup>d</sup> Interference from the  $^{223}\text{Fr}$  155.5 keV  $\gamma$  ray with  $P_\gamma = 0.000038\%$  is considered negligible.

<sup>e</sup> Interference from the  $^{227}\text{Ac}$  159.2 keV  $\gamma$  ray with  $P_\gamma = 0.00055\%$  is considered negligible.

<sup>f</sup> Interference from the  $^{223}\text{Fr}$  444.5 keV  $\gamma$  ray with  $P_\gamma = 0.000015\%$  is considered negligible.

<sup>g</sup> Interference from the  $^{223}\text{Fr}$  537.2 keV  $\gamma$  ray with  $P_\gamma = 0.00007\%$  is present.

<sup>h</sup> Interference from the  $^{227}\text{Th}$  623.8 keV  $\gamma$  ray with  $P_\gamma = 0.00016\%$  is considered negligible.

**Table 8**  
Absolute  $\gamma$ -ray emission probabilities (%) measured in the  $^{219}\text{Rn} \rightarrow ^{215}\text{Po}$  decay.

Energy (keV)	DDEP	JRC	ENEA	CEA	CMI	This work
271.228	11.07 (22)	11.1 (6)	11.4 (5)		11.5 (4)	11.3 (4)
293.56	0.075 (3)	0.065 (3)				0.065 (3)
401.81	6.75 (22)	6.8 (4)	6.98 (30)		7.14 (23)	6.98 (26)
517.6	0.043 (3)	0.046 (3) <sup>i</sup>		0.046 (2) <sup>i</sup>	0.047 (14) <sup>i</sup>	0.046 (2)
676.66	0.018 (2)	0.0208 (12)				0.0208 (12)
891.1	0.0009 (2)	0.0005 (2) <sup>j</sup>				0.0005 (2)

<sup>i</sup> Interference from the  $^{227}\text{Th}$  516.6 keV  $\gamma$  ray with  $P_\gamma = 0.00028\%$  is considered negligible.

<sup>j</sup> Interference from the  $^{227}\text{Th}$  891 keV  $\gamma$  ray with  $P_\gamma = 0.000019\%$  is considered negligible.

**Table 9**  
Absolute  $\gamma$ -emission probabilities (%) measured in the  $^{215}\text{Po} \rightarrow ^{211}\text{Pb}$  decay.

Energy (keV)	DDEP	JRC	ENEA	CEA	CMI	This work
438.9	0.058 (19)	0.0544 (21) <sup>k</sup>		0.0565 (16) <sup>k</sup>	0.073 (13) <sup>k</sup>	0.058 (4)

<sup>k</sup> Interferences from the  $^{227}\text{Ac}$  439.6 keV  $\gamma$  ray with  $P_\gamma = 0.000034\%$  and the  $^{223}\text{Fr}$  439.6 keV with  $P_\gamma = 0.0000042\%$  are considered negligible.

### 2.3. Source covering

The  $^{227}\text{Ac}$  activity of each source can be calculated from the total alpha activity assuming that the  $^{227}\text{Ac}$  and its decay products nuclides are in equilibrium during measurement (denoted as  $^{227}\text{Ac}_{\text{eq}}$ ). It was

apparent from the first measurements that the initial covering with  $2 \times 35 \mu\text{g}/\text{cm}^2$  VYNS foils did not suffice to contain all recoil atoms and the radon gas, thus invalidating the equilibrium assumption. The background count rate increased a hundred times after the measurement but decreased and levelled off after approximately five hours. The

**Table 10**  
Absolute  $\gamma$ -ray emission probabilities (%) measured in the  $^{211}\text{Pb} \rightarrow ^{211}\text{Bi}$  decay.

Energy (keV)	DDEP	JRC	ENEA	CEA	CMI	This work
404.83	3.83 (6)	4.07 (19) <sup>l</sup>	4.22 (18) <sup>l</sup>		4.31 (14) <sup>l</sup>	4.20 (15)
427.15	1.81 (4)	1.91 (9)	1.99 (9)		1.99 (8)	1.96 (7)
429.65	0.008 (3)	0.004 (1)				0.004 (1)
504.07	0.0059 (8)	0.0021 (4)				0.0021 (4)
704.675	0.47 (1)	0.510 (24) <sup>m</sup>	0.527 (24) <sup>m</sup>		0.530 (28) <sup>m</sup>	0.522 (19)
766.68	0.62 (4)				0.781 (26) <sup>n</sup>	0.78 (4)
831.984	3.50 (5)	3.64 (17)	3.75 (16)		3.76 (12)	3.72 (14)
865.92	0.0046 (2)	0.0060 (4)				0.0060 (4)
1014.38	0.0173 (5)	0.012 (5) <sup>r</sup>				0.012 (5)
1080.64	0.0121 (5)	0.0130 (7)				0.0130 (7)
1103.52	0.0047 (7)	0.0036 (3)				0.0036 (3)
1109.509	0.116 (3)	0.119 (6)	0.129 (7)		0.16 (6)	0.125 (8)
1196.33	0.0103 (4)	0.0101 (6)				0.0101 (6)
1234.3	0.0009 (3)	0.00064 (22)				0.00064 (22)
1270.75	0.0068 (12)	0.0066 (4)		0.0071 (3)		0.0069 (3)

<sup>l</sup> Interferences from the  $^{219}\text{Rn}$  405.4 keV  $\gamma$  ray with  $P_\gamma = 0.00025\%$  is considered negligible.

<sup>m</sup> Interferences from the  $^{227}\text{Th}$  704.3 keV  $\gamma$  ray with  $P_\gamma = 0.00008\%$  is considered negligible.

<sup>n</sup> Interferences from the  $^{227}\text{Th}$  439.6 keV  $\gamma$  ray with  $P_\gamma = 0.0003\%$  and the  $^{223}\text{Fr}$  766.64 keV with  $P_\gamma = 0.00031\%$  are considered negligible.

<sup>o</sup> Interference from the  $^{227}\text{Th}$  1015.2 keV  $\gamma$  ray with  $P_\gamma = 0.0000148\%$  is considered negligible.

**Table 11**  
Absolute  $\gamma$ -ray emission probabilities (%) measured in the  $^{211}\text{Bi} \rightarrow ^{207}\text{Tl}$  decay.

Energy (keV)	DDEP	JRC	ENEA	CEA	CMI	This work
351.03	13.00 (19)	13.5 (5) <sup>p</sup>	14.0 (7) <sup>p</sup>		14.1 (5) <sup>p</sup>	13.9 (5)

<sup>p</sup> Interference from the  $^{227}\text{Th}$  (350.54 + 352.61) keV  $\gamma$  rays with  $P_\gamma = 0.12\%$  have been subtracted mathematically.

**Table 12**  
Absolute  $\gamma$ -ray emission probabilities (%) measured in the  $^{207}\text{Tl} \rightarrow ^{207}\text{Pb}$  decay.

Energy (keV)	DDEP	JRC	ENEA	CEA	CMI	This work
897.77	0.263 (9)	0.27 (1) <sup>q</sup>	0.28 (2) <sup>q</sup>			0.28 (2)

<sup>q</sup> Interferences from the  $^{223}\text{Fr}$  (896.7 keV) and  $^{211}\text{Po}$  (897.8 keV)  $\gamma$  rays with  $P_\gamma = 0.016\%$  have been subtracted mathematically.

increase of the background count rate was mainly caused by the  $^{211}\text{Bi}$  ( $T_{1/2} = 2.14$  min) fed by the  $^{211}\text{Pb}$  ( $T_{1/2} = 36.1$  min) (Fig. 3). The sources were later covered with additional VYNS foils, attaching them to the

source disc using acetone vapours, but escape of recoil atoms and Rn was still evident.

Several foil covering strategies were tested to trap the  $^{219}\text{Rn}$  and the recoil atoms in the source, until eventually a practical and easy method was developed. The sources were covered gradually with  $35 \mu\text{g}/\text{cm}^2$  VYNS foils, each applied on the source using a cyanoacrylate glue, one foil at a time, until the background count rate remained constant after the source measurement. Each foil was afterwards heated gently with a hot air blower to attach it completely onto the glass disc. In most of the cases, three foils were adequate to retain the  $^{219}\text{Rn}$  and the recoil atoms. This method proved generally effective, but in few cases the VYNS leaked after a few hours, meaning that the seal was broken. This test verifies the short-term validity of the method only, since radiation damage to the VYNS is expected to make it friable on the long run.

Diffusion of  $^{219}\text{Rn}$  through the VYNS foils was considered insignificant. The diffusion coefficient of Rn in VYNS is less than  $10^{-11} \text{ m}^2/\text{s}$ . In conjunction with its short half-life, the diffusion length is less than 8  $\mu\text{m}$  (Khan, 2015; Keller and Hoffmann, 2000; Pressyanov et al., 2011). A total uncertainty of 0.15 % on the geometrical efficiency (see Table 2) buffers safely any errors due to diffusion. The thickness of VYNS foils were of the order of 60  $\mu\text{m}$  each.

**Table 13**  
Typical relative standard uncertainties (in %,  $k = 1$ ) for the emission probabilities of the  $^{227}\text{Th} \rightarrow ^{223}\text{Ra}$  235.96 keV and 286.09 keV  $\gamma$  rays, as estimated by the individual laboratories.

Component (%) <sup>*</sup>	235.96 keV				286.09 keV			
	JRC	ENEA	CMI	CEA	JRC	ENEA	CMI	CEA
Counting statistics	0.04	0.2	0.1	0.04	0.12	0.54	0.8	0.12
Efficiency	3.6	3	3	1.5	3.6	3	3	1.5
Coincidence summing	3	3	2	0.1	3	3	2	0.2
Source activity	0.55	0.6	0.8	0.9	0.55	0.6	0.8	0.9
Dead Time/pile-up	0.12	< 0.1	0.1	< 0.1	0.12	< 0.1	0.1	< 0.1
<b>Total</b>	<b>4.7</b>	<b>4.3</b>	<b>3.7</b>	<b>2.6</b>	<b>4.7</b>	<b>4.3</b>	<b>3.2</b>	<b>2.6</b>

\* Decay correction during measurement is negligible.

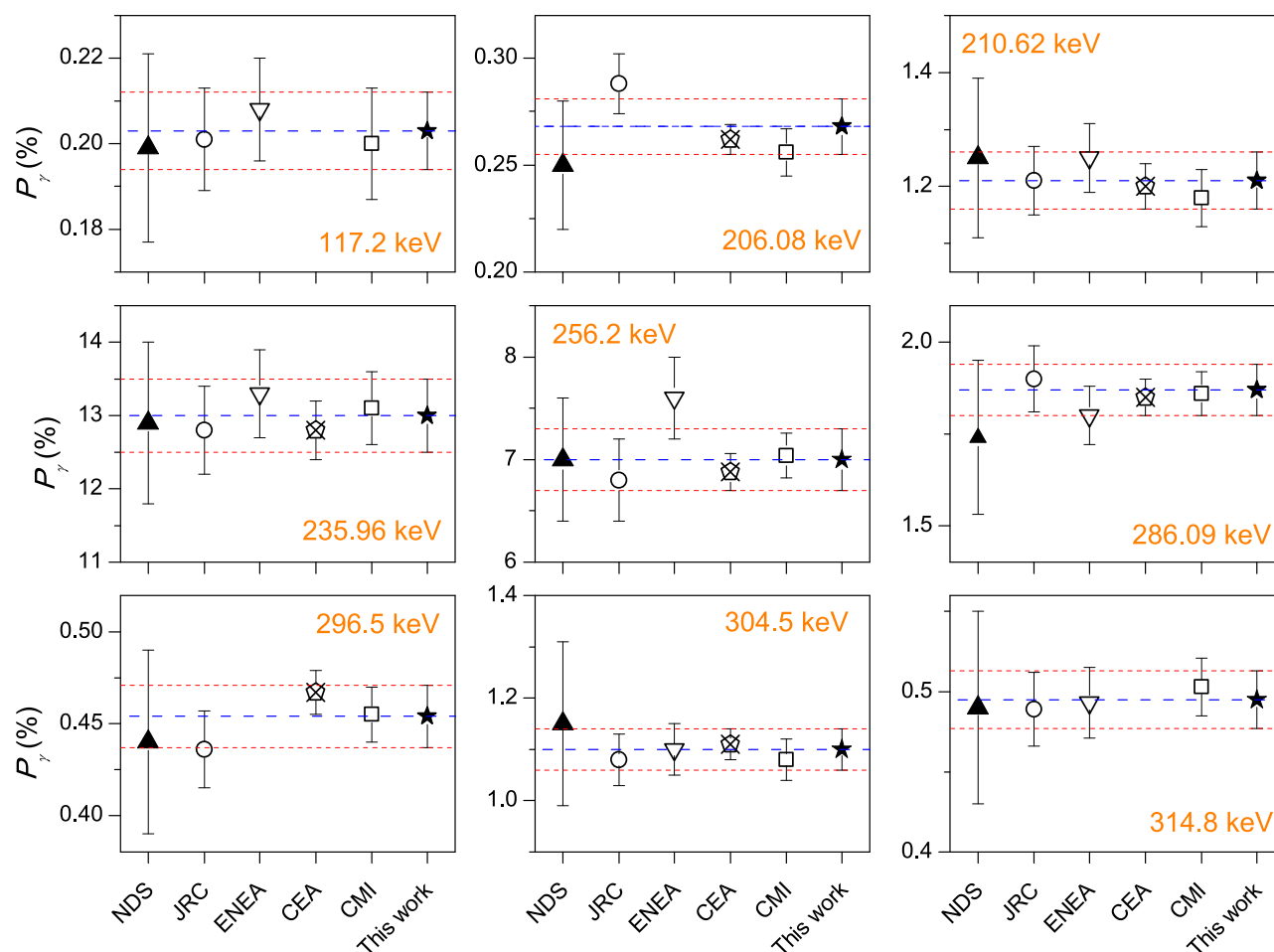


**Fig. 6.** The PMM values (solid lines) of the measured  $^{227}\text{Th}$  absolute emission probabilities for  $\gamma$  rays measured by at least three out of the four laboratories. The standard uncertainties (red dotted lines) of the mean values (blue dashed lines) include a systematic 1 % uncertainty on the CCFs. The evaluated  $P_\gamma$  values from the NDS database (upright black triangles) are included in the graphs for easy comparison. (For interpretation of the references to color in this figure legend, the reader is referred to the web version of this article).

#### 2.4. Sources for $\gamma$ -ray spectrometry

After execution of the activity standardisation measurements, the sources were covered more robustly to facilitate the handling for  $\gamma$ -ray spectrometry measurements and to further prevent material loss from the source. Discs were cut out of polyethylene film of 0.1 mm thickness at the same diameter as the source substrates. They were attached to the top face of the sources, using the same technique as for VYNS foils; they were first glued by applying cyanoacrylate glue at the periphery of the disc and then heated with a hot air blower.

### 3. Activity standardisation

#### 3.1. Alpha counting at defined solid angle

The primary standardisation (Pommé, 2007) of the sources' activities was carried out using a defined solid angle (DSA) alpha counting setup (Pommé and Sibbens, 2008; Pommé, 2015). The detector used

was a passivated implanted planar silicon PIPS<sup>®</sup> detector with a 900 mm<sup>2</sup> active area. The sources were placed at 5 cm distance from the detector. Two baffles (thin metal plates with 29 mm and 64 mm diameter central cut-out) were placed inside the counting chamber to minimise detection of alpha-particles scattered from the inner walls of the counter chamber. The sources were mostly measured at a 0.7 % geometrical efficiency ( $= \text{solid angle}/4\pi$ ). The activity distribution was obtained by digital autoradiography and the source to the detector distance by an optical focusing distance measuring device. Such low efficiency was chosen to minimise the chance for coincident signals from successive decays, in particular to avoid alpha decays being obscured by the system dead time due to decays from a short-lived successor in the decay chain.

The energy window selected for DSA counting was such as to include all the alpha decays of  $^{227}\text{Ac}$  and its daughters, from 2.5 MeV up to 10 MeV. The  $^{227}\text{Ac}$  is considered to be in secular equilibrium with its daughters. The counts below the threshold are accounted for by extrapolation of the low-energy spectrum towards zero energy (Fig. 4).

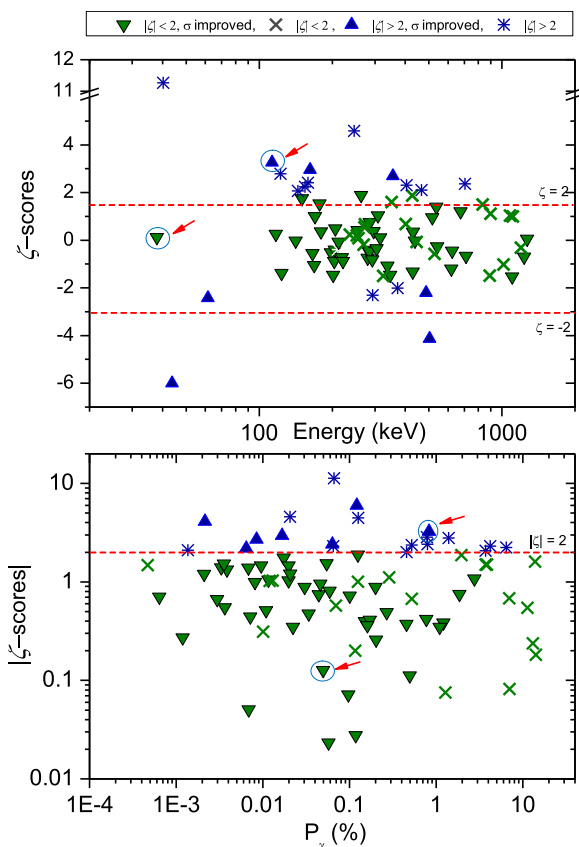


Fig. 7. Comparison of absolute  $\gamma$ -ray emission probabilities from this work with recommended data from the DDEP and the NDS databases using the  $\zeta$ -score. The circled data points indicate emission probabilities for which formerly no uncertainties were assigned.

The standardised activities of the sources used in the project to determine the  $\gamma$ -ray emission probabilities and their associated combined standard uncertainties are summarized in Table 1. A typical uncertainty budget is presented in Table 2.

Drying the sources in open air instead of using a hot plate had as an outcome the formation of comparably large crystals and an increased self-absorption of the alpha particles. Consequently, the number of events was increased by a factor of 1.006–1.013, depending on the source quality, to compensate for the sub-threshold events due to self-absorption. This correction is the main contributor to the total uncertainty of the activity of the sources (see extrapolation uncertainty in Table 2). Additional uncertainty was introduced for non-equilibrium of  $^{227}\text{Ac}$  with its decay products, to account for some recoil atoms escaping from the sources before the adequate covering was applied and for hypothetical losses of Rn which may not show up in the background measurements.

### 3.2. Independent check

The activity of one of the sources (Ac227G1509) was checked by  $\gamma$ -ray spectrometry with high-purity germanium (HPGe) detectors, one above ground and one underground in the Hades facility (Andreotti et al., 2011). The measurements lasted a month each. Emission

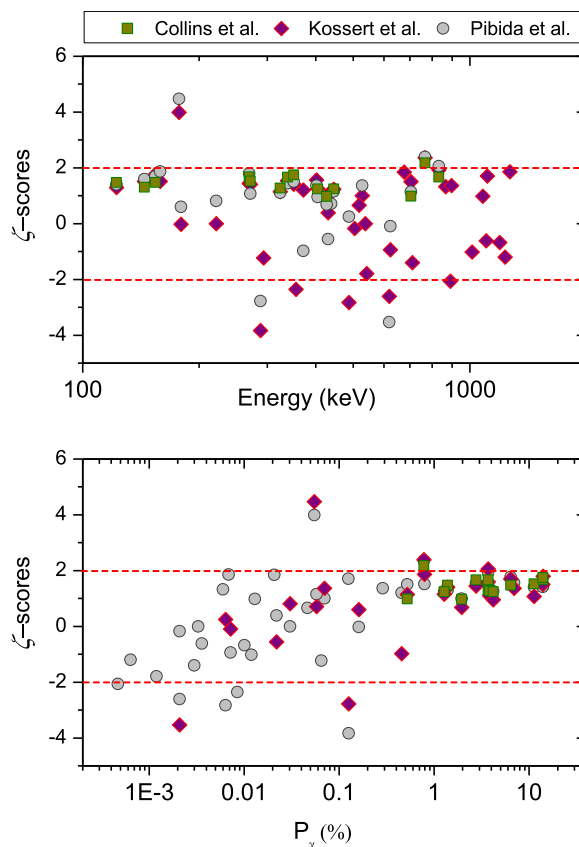


Fig. 8. Comparison of absolute  $\gamma$ -ray emission probabilities from this work with those measured by Pibida (2015), Kossert et al. (2015) and Collins et al. (2015b) using the  $\zeta$ -score.

probabilities from the DDEP and NDS databases were used for the calculation of the activities of the  $^{227}\text{Ac}$  decay products  $^{223}\text{Ra}$ ,  $^{219}\text{Rn}$ ,  $^{211}\text{Pb}$  and  $^{211}\text{Bi}$  and the selected peaks are identified in the  $^{227}\text{Ac}$   $\gamma$ -ray spectrum of Fig. 5. Activities determined from both  $\gamma$ -ray spectrometry measurements agreed within one standard uncertainty with results from the alpha-counting measurement (Table 3). This can be used only as a rough check, due to the 5 % relative uncertainty on the measurements of  $\gamma$ -ray spectrometry.

### 3.3. Impurities check

Via the production of  $^{227}\text{Ac}$  from the irradiation of  $^{226}\text{Ra}$ , minor traces of  $^{226}\text{Ra}$  could be present in the obtained solution. One of the produced sources was measured using  $\gamma$ -ray spectrometry with a HPGe detector to identify possible traces of  $^{226}\text{Ra}$ . Due to the vast number of  $\gamma$ -ray lines in the spectrum, the 242 keV  $\gamma$ -ray line following the decay of  $^{214}\text{Pb}$  was selected to quantify the amount of  $^{226}\text{Ra}$ . The activity of  $^{226}\text{Ra}$  in the produced sources was less than 0.03 % of their total activity.

## 4. $\gamma$ -ray spectrometry

### 4.1. Method

The participating laboratories received one  $^{227}\text{Ac}_{\text{eq}}$  source each. All

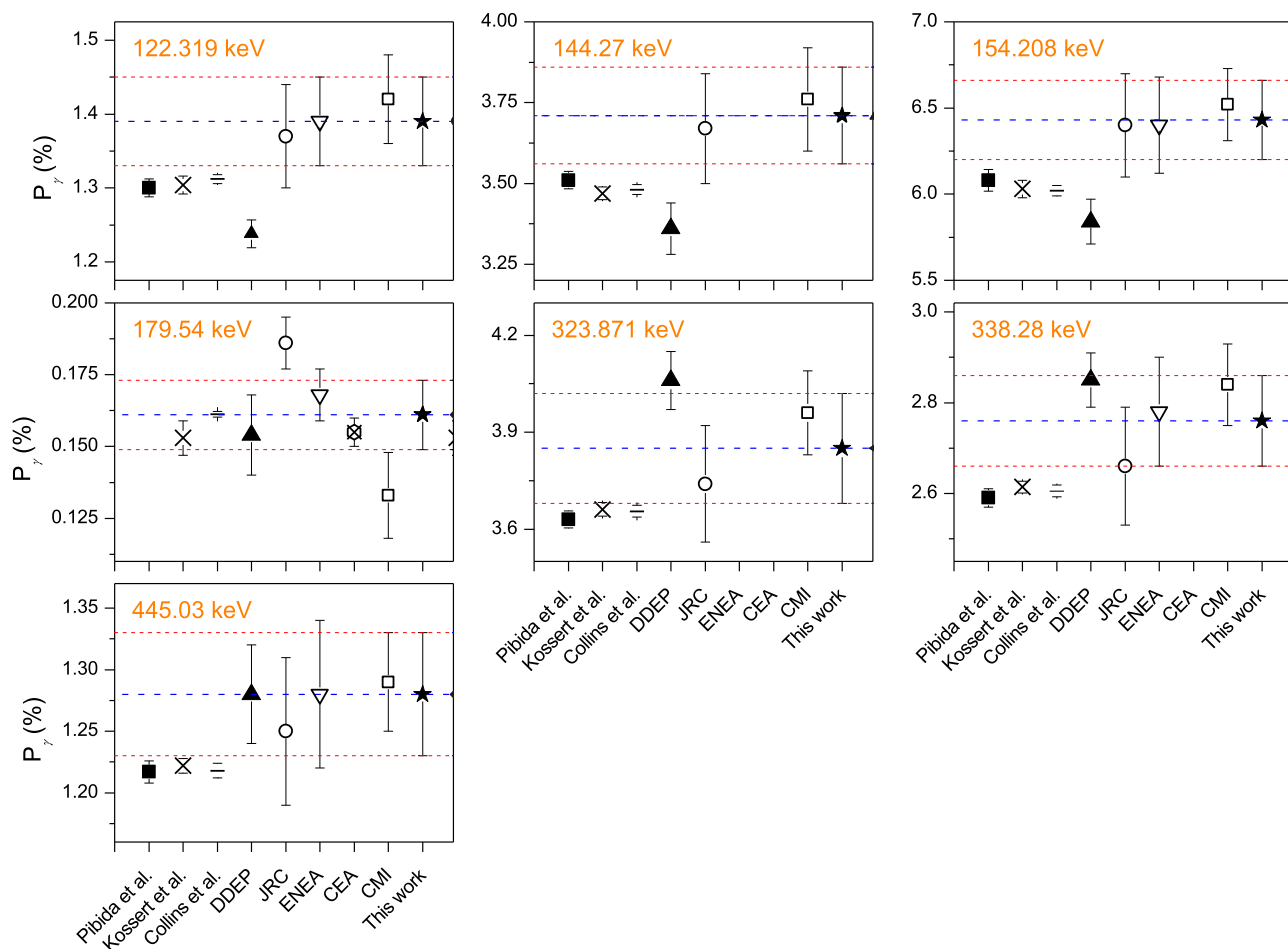


Fig. 9. Absolute  $\gamma$ -ray emission probabilities from this work and those measured by Pibida (2015), Kossert et al. (2015) and Collins et al. (2015b) for the  $^{223}\text{Ra} \rightarrow ^{219}\text{Rn}$  decay.

sources were measured with HPGe detectors calibrated for the full energy peak (FEP) detection efficiency  $\epsilon(E_\gamma)$  as a function of the  $\gamma$ -ray energy. Most of the laboratories calculated a transfer efficiency correction factor by Monte Carlo simulations, thus adjusting the measured  $\epsilon(E_\gamma)$  curve to account for the differences in geometry and matrix between the calibration sources and the  $^{227}\text{Ac}_{\text{eq}}$  sources. True coincidence summing correction factors (CCFs) were calculated by all participants. Due to the low branching ratio of  $^{227}\text{Ac} \rightarrow ^{223}\text{Fr}$ ,  $\gamma$  rays emitted in the decays of  $^{223}\text{Fr} \rightarrow ^{219}\text{At} \rightarrow ^{215}\text{Bi} \rightarrow ^{215}\text{Po}$  were neglected from the data analysis. Details on the experimental methods are presented in Table 4. Typical uncertainties associated with the  $\gamma$ -ray spectrometry technique have been discussed by Lépy et al. (2015).

#### 4.2. Results

Gamma rays reported in the DDEP database for  $^{227}\text{Ac}$ ,  $^{223}\text{Ra}$ ,  $^{219}\text{Rn}$ ,  $^{215}\text{Po}$ ,  $^{211}\text{Pb}$ ,  $^{211}\text{Bi}$  and  $^{207}\text{Tl}$ , and those included in the decay data evaluation published in NDS for  $^{227}\text{Th}$  (Browne, 2011) were considered in the analysis of the spectra.

An overview of the reported  $\gamma$ -ray emission probabilities from this work is presented in Tables 5–12 and a typical uncertainty budget in

Table 13. For  $\gamma$ -ray lines on which more than one laboratory reported a result, the  $\gamma$ -ray emission probabilities were combined into a final value by calculating the power-moderated mean or PMM (Pommé and Keighley 2015). Emission probabilities for peaks suffering from spectral interferences not resolved by the fitting software were not reported, unless explicitly stated in the table. For the rest of the  $\gamma$ -ray lines interferences are considered negligible. As seen in Table 13, each laboratory estimated the uncertainty on the CCFs in a different way. To avoid that differences in the uncertainty assessments would having a large impact on the relative weighting factors, this CCF uncertainty component was initially not taken into account for the calculation of the PMM. Thus, a more stable mean value is obtained and this systematic error was taken into account by adding a 3 % uncertainty in quadrature to the PMM uncertainty. The results are generally intermediate between arithmetic and weighted mean, depending on the level of mutual consistency. A coverage factor of  $k = 2$  was selected to identify extreme data and a default value was used for the power of the weighting factors ( $\alpha = 2-3/N$ ). Fig. 6 shows the PMM for the  $^{227}\text{Th}$   $\gamma$ -ray lines for which at least three out of the four laboratories reported an emission probability.

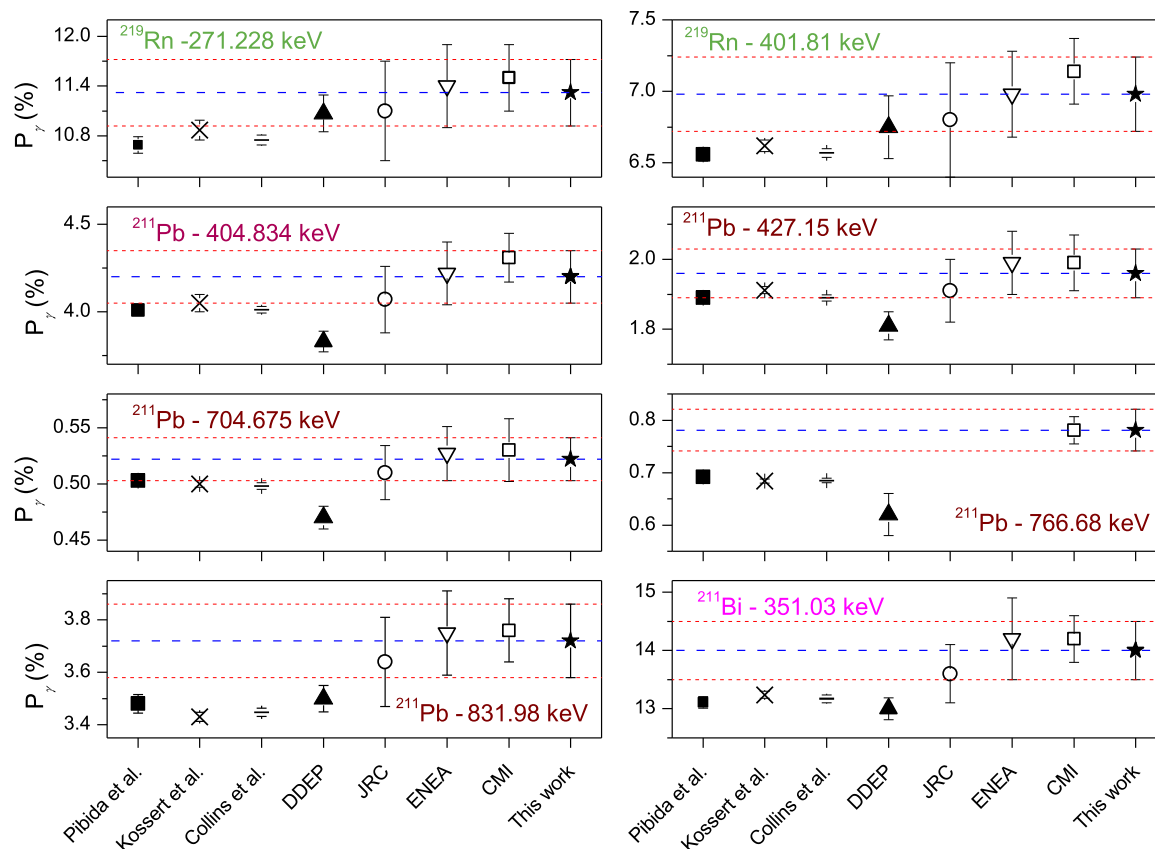


Fig. 10. Absolute  $\gamma$ -ray emission probabilities from this work and those measured by Pibida (2015), Kossert et al. (2015) and Collins et al. (2015b) for the  $^{219}\text{Rn}$  down to  $^{207}\text{Pb}$  decay.

## 5. Discussion

When excluding the reported sum peaks from the evaluation, 64 out of the 84 measured  $P_\gamma$  values reported in this work (Tables 5–13) agree with the evaluated data from the DDEP and NDS. In addition, uncertainties on the emission probabilities for 45  $\gamma$  rays have been reduced. To compare the  $P_\gamma$  from this work with the evaluated data, the  $\zeta$  score is calculated:

$$\zeta = \frac{P_y^m - P_y^{ev}}{\sqrt{u_m^2 + u_{ev}^2}}$$

The index  $m$  refers to values measured in this work and  $ev$  to evaluated data.  $P_\gamma$  and  $u$  are the  $\gamma$ -emission probabilities and their standard uncertainties. Assuming a normal distribution, a value of  $|\zeta| < 2$  corresponds to a 95 % confidence interval.

A graphical representation of the above criterion is shown in Fig. 7. It is evident that most measured values are in agreement with the evaluated data, however exceptions do exist. For example, the  $P_\gamma$  for the  $^{227}\text{Th} \rightarrow ^{223}\text{Ra}$  40.2 keV  $\gamma$  ray from NDS (0.015(4) %) and this work (0.066(5) %) do not match ( $\zeta = 11$ ). It should be noted though that the NDS value is extracted from only two studies held in the sixties lacking uncertainty assignment (Briançon et al., 1968; Davidson, Connor, 1970). Disagreement exists as well for the  $^{227}\text{Th} \rightarrow ^{223}\text{Ra}$  113.11 keV

$\gamma$  ray ( $\zeta = 3$ ). Although there is a discrepancy with the value from (Briançon and Walen, 1971), there is good agreement with the more recent measurement by Abdul-Hadi et al. (1993).

A comparison has also been made with the most recently measured  $\gamma$ -ray emission probabilities in the decay of  $^{223}\text{Ra} \rightarrow ^{219}\text{Rn}$ ,  $^{219}\text{Rn} \rightarrow ^{215}\text{Po}$ ,  $^{211}\text{Pb} \rightarrow ^{211}\text{Bi}$ , and  $^{211}\text{Bi} \rightarrow ^{207}\text{Tl}$  by Pibida (2015), Kossert et al. (2015) and Collins et al. (2015b). These are not included yet in the evaluations by DDEP or NDS. Applying the  $|\zeta| < 2$  criterion, the absolute  $\gamma$ -ray emission probabilities are in most of the cases in agreement with the values published in this work (Fig. 8). A direct comparison of absolute emission probabilities is shown for various  $\gamma$ -ray energies in Fig. 9 and Fig. 10. The estimated uncertainties in this work are significantly higher than in the three recent works, where uncertainties of 1 % or less are quoted.

It is evident that the absolute emission probabilities reported in this work are consistently higher than the most recently published ones. An explanation could be a possible underestimation of the activity standardisation of the sources. The most probable reason could be either the loss of Rn gas or the underestimation of the self-absorption correction.

The exclusion of the first was realised in two ways. Firstly, the background has been checked before and after each activity measurement and it remained constant proving the containment of Rn on the source substrate within the measuring time. Secondly, the experimental

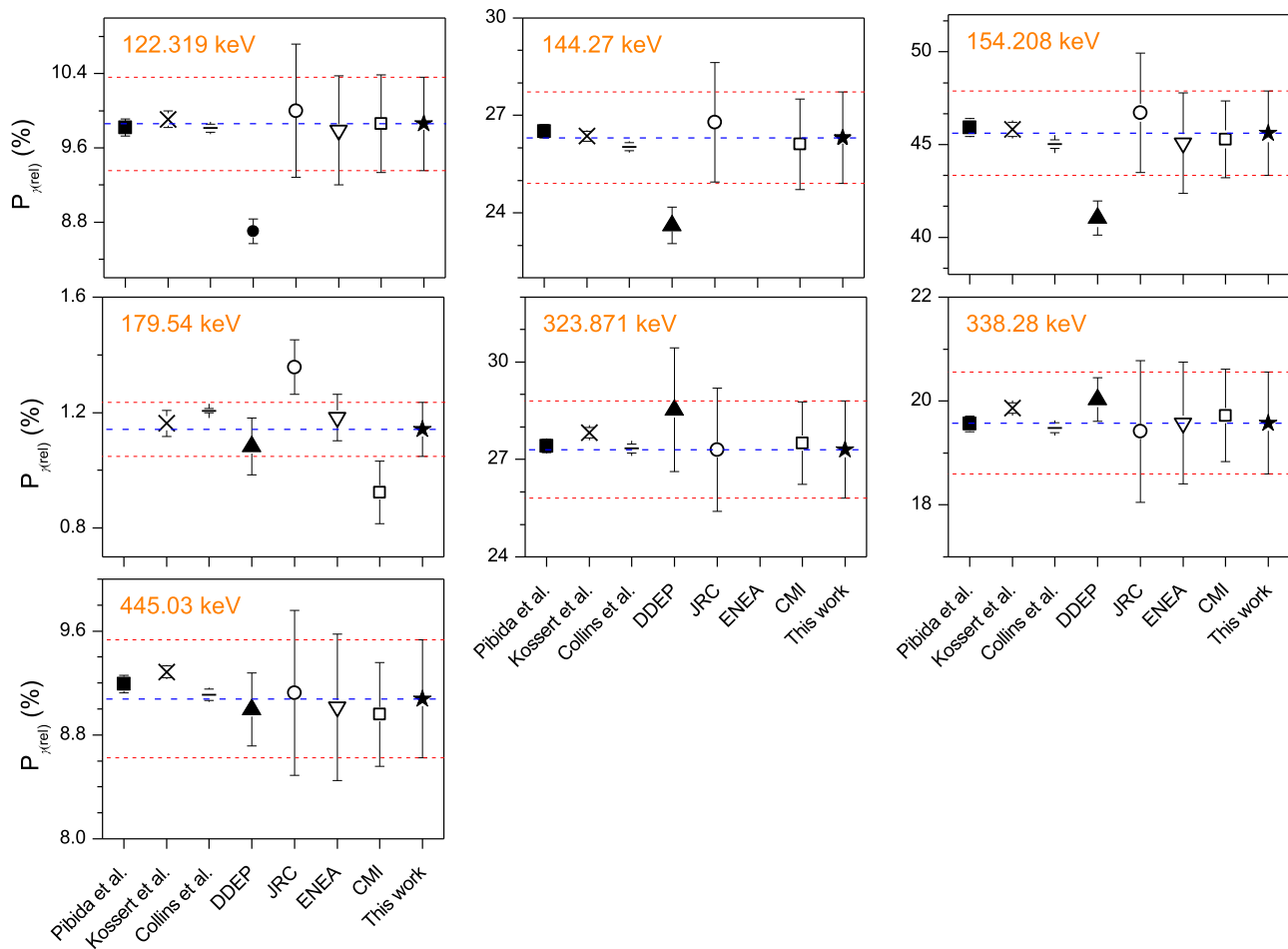


Fig. 11. Relative  $\gamma$ -ray emission probabilities from this work and those measured by Pibida (2015), Kossert et al. (2015) and Collins et al. (2015b) for the  $^{223}\text{Ra} \rightarrow ^{219}\text{Rn}$  decay.

ratio of counts of the  $^{227}\text{Ac}$ - $^{227}\text{Th}$ - $^{223}\text{Ra}$  to the rest of the decay products,  $^{219}\text{Rn}$  down to  $^{207}\text{Pb}$ , was investigated. If  $^{219}\text{Rn}$  was escaping, it would be manifested by a decrease in the integral of the measured counts from the decay products  $^{211}\text{Bi}$ ,  $^{219}\text{Rn}$  and  $^{215}\text{Po}$  compared to theory assuming equilibrium. The alpha spectra obtained for each source were fitted with the deconvolution software 'BEST' (Pommé and Marroyo, 2015). The experimental and theoretical ratios of the integral counts of  $^{227}\text{Ac}$ ,  $^{227}\text{Th}$  and  $^{223}\text{Ra}$  to  $^{211}\text{Bi}$ ,  $^{211}\text{Po}$ ,  $^{219}\text{Rn}$  and  $^{215}\text{Po}$  were calculated and compared. There was no significant difference between the two ratios within a 2 % absolute uncertainty.

On the other hand, the formation of comparably large crystals after drying the sources freely in open air increased the self-absorption of the alpha particles. It affected also the correction for the counts lost below the threshold which is done by extrapolating the spectrum to zero energy (Fig. 4). Because of the bad quality of the alpha sources for primary standardisation one of the two aforementioned corrections might not have been fully accounted. For that reason, and to exclude the activity as a parameter in the determination of the absolute emission probabilities (Fig. 9, Fig. 10), the relative emission probabilities ( $P_{\gamma(\text{rel})}$ ) to the  $^{223}\text{Ra}$  269.3 keV  $\gamma$ -ray emission probability for each laboratory are shown in Fig. 11 and Fig. 12. The relative emission probabilities of

this work are in a very good agreement with those by Pibida et al., Kossert et al. and Collins et al.. This is clearly depicted by comparing Fig. 8 with its corresponding graph of  $\zeta$ -scores for the relative emission probabilities (Fig. 13).

## 6. Conclusions

The  $\gamma$ -ray emission probabilities of  $^{227}\text{Ac}$  and its decay products were measured by  $\gamma$ -ray spectrometry with HPGe detectors. Emission probabilities from 87  $\gamma$ -ray lines are reported in this work; the majority agree within uncertainties with the DDEP/NDS recommended values and with the most recently published values in the literature. The primary standardisation of activity of the measured sources and the completeness of the uncertainty budget provided by the participating laboratories contribute to the SI-traceability of the provided reference decay data. However, there is doubt on the accuracy of the absolute standardisation due to self-absorption problems. Nevertheless, it was clear that the relative  $\gamma$ -ray emission probabilities of this work were in better agreement with the most recent published ones compared to the absolute emission probabilities.

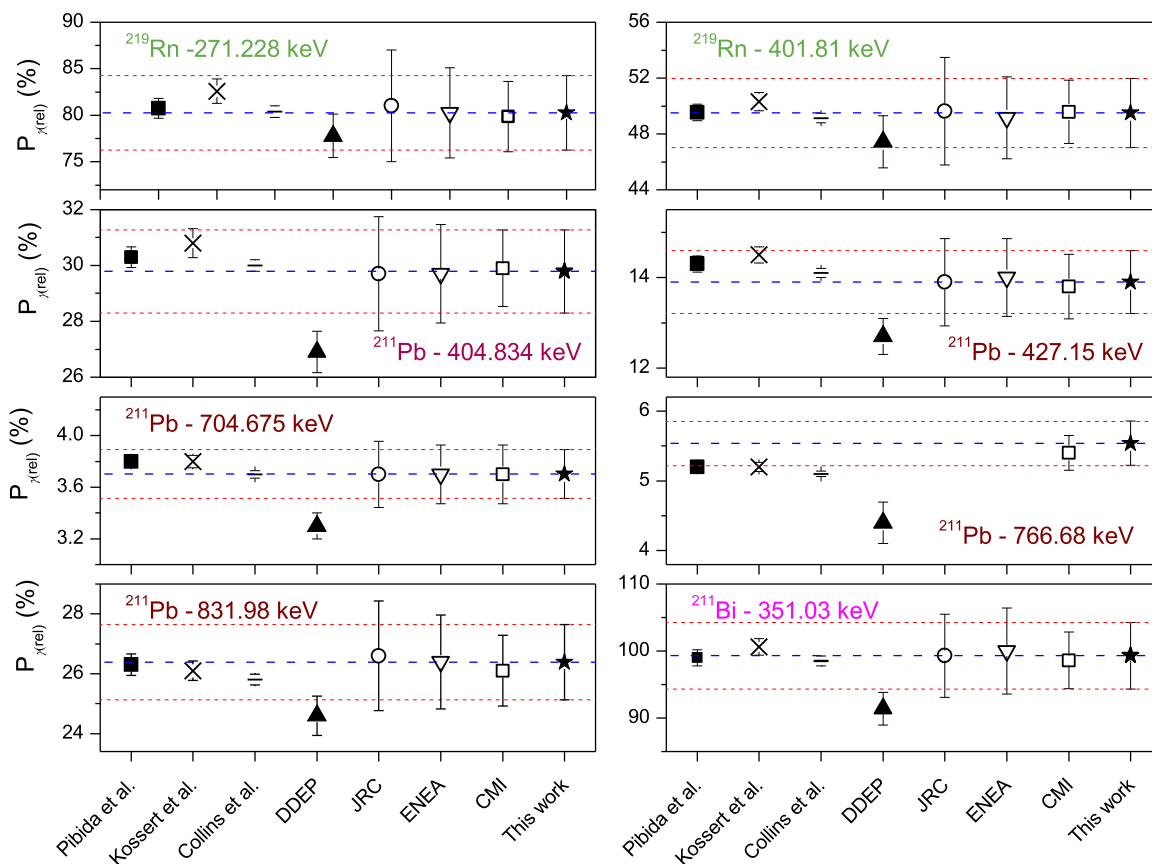


Fig. 12. Relative  $\gamma$ -ray emission probabilities values from this work and those measured by Pibida (2015), Kossert et al. (2015) and Collins et al. (2015b) for the  $^{219}\text{Rn}$  down to  $^{207}\text{Pb}$  decay.

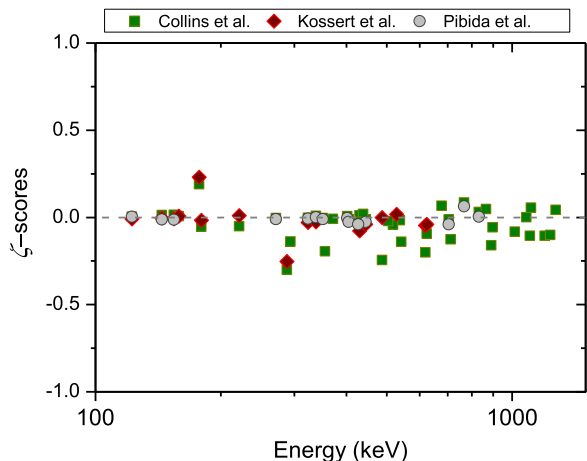


Fig. 13. Comparison of the relative  $\gamma$ -ray emission probabilities values from this work with those measured by Pibida (2015), Kossert et al. (2015) and Collins et al. (2015b) for the  $^{219}\text{Rn}$  down to  $^{207}\text{Pb}$  decay using the  $\zeta$ -score.

**Acknowledgments**

This work has been supported by the European Metrology Research Programme (EMRP), JRP-Contract IND57 MetroNORM ([www.emrponline.eu](http://www.emrponline.eu)). The EMRP is jointly funded by the EMRP participating countries within EURAMET and the European Union.

The authors would like to thank Gerd Marissens, Jan Paepen and Heiko Stroh for their technical support.

**References**

Abdul-Hadi, A., Barci, V., Weiss, B., Maria, H., Ardisson, G., 1993.  $^{223}\text{Ra}$  levels fed in the  $^{223}\text{Fr}$   $\beta$  decay. *Phys. Rev. C* 47, 94–109.

Andreotti, E., Hult, M., Gonzalez de Orduña, R., Marissens, G., Mihailescu, M., Wätjen, U., Van Marcke, P., 2011. Status of underground radioactivity measurements in HADES. In: *Proceeding of the 3rd International Conference 'Current Problems in Nuclear Physics and Atomic Energy'*. 7-12 June 2010. pp. 601–605.

Apostolidis, C., Molinet, R., Rasmussen, G., Morgenstern, A., 2005. Production of Ac-225 from Th-229 for targeted  $\alpha$  therapy. *Anal. Chem.* 77, 6288–6291.

Bergeron, D.E., Fitzgerald, R., 2015. Two determinations of the  $^{223}\text{Ra}$  half-life. *Appl. Rad. Isot.* 102, 74–80.

Briançon, C., Leang, C.F., Walen, R., 1968. Etude du spectre  $\gamma$  emis par le Radium-223 et ses derives. *Compt. Rend.* 266B, 1533.

Briançon, C., Walen, R., 1971. Scema de niveaux de  $^{223}\text{Ra}$  III. Etude des coincidences  $\gamma * \gamma$  et des vies moyennes. *J.Phys.* 32, 381.

Browne, E., 2011. Nuclear data sheets for A = 215, 219, 223, 227, 231. *Nucl. Data Sh.* 93, 763–1062.

Collins, S.M., Pearce, A.K., Ferreira, K.M., Fenwick, A.J., Regan, P.H., Keightley, J.D., 2015a. Direct measurement of the half-life of  $^{223}\text{Ra}$ . *Appl. Rad. Isot.* 99, 46–53.

Collins, S.M., Pearce, A.K., Regan, P.H., Keightley, J.D., 2015b. Precise measurements of the absolute  $\gamma$ -ray emission probabilities of  $^{223}\text{Ra}$  and decay progeny in equilibrium. *Appl. Rad. Isot.* 102, 15–28.

Collins, S.M., Pommé, S., Jerome, S.M., Ferreira, K.M., Regan, P.H., Pearce, A.K., 2015c. The half-life of  $^{227}\text{Th}$  by direct and indirect measurements. *Appl. Rad. Isot.* 104, 203–211.

Davidson, W.F., Connor, R.D., 1970. The decay of  $^{223}\text{Ra}$  and its daughter products: (ii). The decay of  $^{219}\text{Rn}$  and  $^{215}\text{Po}$ . *Nucl. Phys. A* 149, 385–391.

DDEP, 2004–2016. Table of Radionuclides, Vol. 1-8, Monographie BIPM-5 BIPM, Sèvres, website: <http://www.lnhb.fr/nuclear-data/nuclear-data-table/>.

EURATOM, 2014. Council Directive 2013/59/EURATOM, Official Journal of the European Union, 17.1.2014, L13/1-73.

Goorley, T., James, M., Booth, T., Brown, F., Bull, J., Cox, L.J., Durkee, J., Elson, J., Fensin, M., Forster, R.A., Hendricks, J., Hughes, H.G., Johns, R., Kiedrowski, B., Martz, R., Mashnik, S., McKinney, G., Pelowitz, D., Prael, R., Sweezy, J., Waters, L., Wilcox, T., Zukaitis, T., 2012. Initial MCNP6 release overview. *Nucl. Technol.* 180,

- 298–315.
- Hindi, M.M., Adelberger, E.G., Kellogg, S.E., Murakami, T., 1988. Search for the I-forbidden beta decay  $^{207}\text{Tl} \rightarrow ^{207}\text{Pb}$  (570 keV). *Phys. Rev. C* 38, 1370–1376.
- Humm, J.L., Sartor, O., Parker, C., Bruland, O.S., Macklis, R., 2015. Radium-223 in the treatment of osteoblastic metastases: a critical clinical review. *Int. J. Radiat. Oncol. Biol. Phys.* 91, 898–906.
- Kawrakow, I., Mainegra-Hing, E., Rogers, W.O., Tessier, D., F., R. B. Walters. B., 2015. The EGSnrc code system: Monte Carlo simulation of electron and photon transport. Technical Report PIRS-701, National Research Council, Canada.
- Keightley, J., Pearce, A., Fenwick, A., Collins, S., Ferreira, K., Johansson, L., 2015. Standardisation of  $^{223}\text{Ra}$  by liquid scintillation counting techniques and comparison with secondary measurements. *Appl. Rad. Isot.* 95, 114–121.
- Khan, M.S.A., 2015. Study of radon gas diffusion and its permeability through some building construction material by using SSNTD technique. *Int. J. Sci. Res.* 6, 2319–7064.
- Keller, G., Hoffmann, B., 2000. The radon diffusion length as a criterion for the radon tightness. *Int. Nucl. Inf. Syst.* 32, 1–4 (P-1b-52).
- Kondev, F., McCutchan, E., Singh, B., Tuli, J., 2016. Nuclear Data Sheets for A = 227. *Nucl. Data Sh.* 132, 257–354.
- Kossert, K., Bokeloh, K., Dersch, R., Nähle, O., 2015. Activity determination of  $^{227}\text{Ac}$  and  $^{223}\text{Ra}$  by means of liquid scintillation counting and determination of nuclear decay data. *Appl. Rad. Isot.* 95, 143–152.
- Kratochwil, C., Bruchertseifer, F., Giesel, F.L., Weis, M., Verburg, F.A., Mottaghy, F., Kopka, K., Apostolidis, C., Haberkorn, U., Morgenstern, A., 2016.  $^{225}\text{Ac}$ -PSMA-617 for PSMA-targeted  $\alpha$ -radiation therapy of metastatic castration-resistant prostate cancer. *J. Nucl. Med.* 57, 1941–1944.
- Lee, J.Y., 2013. Nuclear Data Sheets for A = 215. *Nucl. Data Sh.* 114, 2023–2078.
- Lépy, M.-C., Pearce, A., Sima, O., 2015. Uncertainties in gamma-ray spectrometry. *Metrologia* 52, S123–S145 (Corrigendum, *Metrologia* 54, 883).
- Liang, C.F., Paris, P., Sheline, R.K., 1999. Configurations and level structure of  $^{215}\text{Po}$ . *Phys. Rev. C* 59, 648–654.
- LNHB, 2008. Logiciel d'ajustement des courbes de rendement AÇORES, Note Technique, LNHB 2008/45.
- Marouli, M., Lutter, G., Pommé, S., Van Ammel, R., Hult, M., Richter, S., Eykens, R., Peyrés, V., García-Torano, E., Dryák, P., Mazánová, M., Carconi, P., 2018. Measurement of absolute  $\gamma$ -ray emission probabilities in the decay of  $^{235}\text{U}$ . *Appl. Rad. Isot.* 132, 72–78.
- Marouli, M., Pommé, S., Paepen, J., Van Ammel, R., Jobbágy, V., Dirican, A., Suliman, G., Stroh, H., Apostolidis, C., Abbas, K., Morgenstern, A., 2012. High-resolution alpha-particle spectrometry of the  $^{230}\text{U}$  decay series. *Appl. Rad. Isot.* 70, 1900–1906.
- Marouli, M., Suliman, G., Pommé, S., Van Ammel, R., Jobbágy, V., Stroh, H., Dikmen, H., Paepen, J., Dirican, A., Bruchertseifer, F., Apostolidis, C., Morgenstern, A., 2013. Decay data measurements on  $^{213}\text{Bi}$  using recoil atoms. *Appl. Rad. Isot.* 74, 123–127.
- Momeni, M.H., 1982. Analyses of uranium and actinium gamma spectra: an application to measurements of environmental contamination. *Nucl. Instrum. Methods* 193, 185–190.
- Pibida, L., 2015. Determination of photon emission probabilities for the main gamma-rays of  $^{223}\text{Ra}$  in equilibrium with its progeny. *Appl. Rad. Isot.* 101, 15–19.
- Piton, F., Lépy, M.-C., Bé, M.-M., Plagnard, J., 2000. Efficiency transfer and coincidence summing corrections for  $\gamma$ -ray spectrometry. *Appl. Rad. Isot.* 52, 791–795.
- Pommé, S., 2007. Methods for primary standardization of activity. *Metrologia* 44, S17–S26.
- Pommé, S., Sibbens, G., 2008. Alpha-particle counting and spectrometry in a primary standardisation laboratory. *Acta Chim. Slov.* 52, 111–119.
- Pommé, S., Altitzoglou, T., Van Ammel, R., Suliman, G., Marouli, M., Jobbágy, V., Paepen, J., Stroh, H., Apostolidis, C., Abbas, K., Morgenstern, A., 2012a. Measurement of the  $^{230}\text{U}$  half-life. *Appl. Rad. Isot.* 70, 1900–1906.
- Pommé, S., Suliman, G., Marouli, M., Van Ammel, R., M., Jobbágy, V., Paepen, J., Stroh, H., Apostolidis, C., Abbas, K., Morgenstern, A., 2012b. Measurement of the  $^{226}\text{Th}$  and  $^{222}\text{Ra}$  half-lives. *Appl. Rad. Isot.* 70, 1913–1918.
- Pommé, S., Marouli, M., Suliman, G., Dimen, H., Van Ammel, R., Jobbágy, V., Dirican, A., Stroh, H., Paepen, J., Bruchertseifer, F., Apostolidis, C., Morgenstern, A., 2012c. Measurement of the  $^{225}\text{Ac}$  half-life. *Appl. Rad. Isot.* 70, 2608–2614.
- Pommé, S., 2015. The uncertainty of counting at a defined solid angle. *Metrologia* 52, S73–S85.
- Pommé, S., Marroyo, C., 2015. Improved peak shape fitting in alpha spectra. *Appl. Rad. Isot.* 96, 148–153.
- Pommé, S., Keightley, J., 2015. Determination of a reference value and its uncertainty through a power-moderated mean. *Metrologia* 52, S200–S212.
- Pommé, S., Collins, S.M., Harms, A.V., Jerome, S., 2016. Fundamental uncertainty equations for nuclear dating applied to the  $^{140}\text{Ba}$ ,  $^{140}\text{La}$  and  $^{227}\text{Th}$ ,  $^{223}\text{Ra}$  chronometers. *J. Env. Rad.* 162–163, 358–370.
- Pressyanov, D., Georgiev, S., Dimitrova, I., Mitev, K., Boshkova, T., 2011. Determination of the diffusion coefficient and solubility of radon in plastics. *Rad. Prot. Dos.* 145, 123–126.
- SCK•CEN, 2015. Highlights. <[http://www.sckcen.be/News/20160608\\_2015\\_Highlights](http://www.sckcen.be/News/20160608_2015_Highlights)> (accessed in June 2016).
- Seidl, C., 2014. Radioimmunotherapy with  $\alpha$ -particle-emitting radionuclides. *Immunotherapy* 6, 431–458.
- Sima, O., Arnold, D., Dovlete, C., 2001. GESPECOR – a versatile tool in gamma ray spectrometry. *J. Radioanal. Nucl. Chem.* 248 (2), 359–364.
- Suliman, G., Pommé, S., Marouli, M., Van Ammel, R., Jobbágy, V., Paepen, J., Stroh, H., Apostolidis, C., Abbas, K., Morgenstern, A., 2012. Measurements of the half-life of  $^{214}\text{Po}$  and  $^{218}\text{Rn}$  using digital electronics. *Appl. Rad. Isot.* 70, 1907–1912.
- Suliman, G., Pommé, S., Marouli, M., Van Ammel, R., Stroh, H., Jobbágy, V., Paepen, J., Dirican, A., Bruchertseifer, F., Apostolidis, C., Morgenstern, A., 2013. Half-lives of  $^{221}\text{Fr}$ ,  $^{217}\text{At}$ ,  $^{213}\text{Bi}$ ,  $^{213}\text{Po}$  and  $^{209}\text{Pb}$  from the  $^{225}\text{Ac}$  decay series. *Appl. Rad. Isot.* 77, 32–37.
- Van Ammel, R., Eykens, S., Eykens, R., Pommé, S., 2011. Preparation of drop-deposited quantitative uranium sources with low self-absorption. *Nucl. Instr. Methods A* 652, 76–78.
- Zielinska, B., Apostolidis, C., Bruchertseifer, F., Morgenstern, A., 2007. An improved method for the production of Ac-225/Bi-213 from Th-229 for targeted alpha therapy. *Solv. Extr. I. Exch.* 25, 339–349.
- Zimmerman, B.E., Bergeron, D.E., Cessna, J.T., Fitzgerald, R., Pibida, L., 2015. Revision of the NIST standard for  $^{223}\text{Ra}$ : new measurements and review of 2008 data. *J. Res. Nat. Inst. Stand. Technol.* 120, 37–57.